JOURNAL OF NANO- AND ELECTRONIC PHYSICS
Vol. **12** No 2, 02024(3pp) (2020)

ЖУРНАЛ НАНО- ТА ЕЛЕКТРОННОЇ ФІЗИКИ
Том **12** № 2, 02024(3cc) (2020)

Tin Oxide Nanostructure Fabricated by Thermal Evaporation as Potential NO_2 Sensor

S.M. Ingole[1,2], Y.H. Navale[1], A.S. Salunkh[1], M.A. Chougule[1], G.D. Khuspe[1], V.B. Patil[1,*]

[1] *Functional Materials Research Laboratory, P.A.H. School of Physical Sciences, Solapur University, Solapur 413255, India*
[2] *Arts,Commerce and Science College Onde, Palghar 401605, India*

(Received 15 February 2020; revised manuscript received 15 April 2020; published online 25 April 2020)

Tin oxide (SnO_2) gas sensor has been fabricated on glass substrate by using thermal evaporation and further characterize by scanning electron microscopy, atomic force microscopy and EDAX analysis for confirming its morphology and composition. The chemiresistive gas sensing performance of SnO_2 films were studied towards various oxidizing and reducing gases. The experimental results reveal that, SnO_2 films were vastly sensitive and selective towards NO_2 gas than other test gases. SnO_2 sensor exhibit maximum response of 160 % for 100 ppm NO_2 gas with very fast response time at optimal operating 200 °C temperature. The SnO_2 sensor manifests remarkably enhanced sensing performance, including fast response and recovery time, high sensitivity, and good stability, suggests of the promising application in the NO_2 gas sensing field.

Keywords: SnO_2, Thermal evaporation, SEM, AFM, NO_2 sensor.

DOI: 10.21272/jnep.12(2).02024 PACS numbers: 64.70.ph, 64.70.fm, 07.07.Df

1. INTRODUCTION

Solid-state *n*-type semiconductors, in general metal oxides and tin dioxide (SnO_2) in demanding, have been extensively exploited as gas sensors. Commercially existing gas sensors that generally operate in the range of 100 and 400 °C temperatures are made mainly of microcrystalline SnO_2 thin films and widely used for detection of harmful gases down to several parts per million (ppm) concentrations [1]. Metal oxide semiconductor gas sensor mechanism is based on their change in resistance caused by different gas exposures such as reducing or oxidizing gases. Solid-state gas sensors have extensive applications in medical diagnosis, semiconductor processing, environmental sensing, national security and personal safety [2].

There are several techniques reported in the literature to develop SnO_2 thin film sensor namely, sol-gel [3], spray pyrolysis [4], thermal evaporation [5], RF magnetron co-sputtering [6], reactive electron beam evaporation [7], CVD [8] etc. In present work, we reported the thin film sensor was synthesized by thermal evaporation technique. Since this method is simple, efficient and effective in producing nanostructures with high surface-to-volume ratio and films of high purity can be obtained [9-11].

Synthesized SnO_2 sensor films were characterized by Raman, scanning electron microscopy (SEM), EDAX, and atomic force microscopy (AFM). The response of film was tested towards to different gases. The gas sensing outcomes reveals that the SnO_2 film is capable to detect the toxic NO_2 gas.

2. EXPERIMENTAL ASPECTS

2.1 Synthesis of SnO_2 Sensor Film

The SnO_2 sensor films were fabricated by using high vacuum thermal coating unit. For synthesis of SnO_2, Sn powder with high purity 99.99 % Aldrich make was used as a source material, at first Sn powder was kept in molybdenum boat located in a high vacuum compartment which is coupled to a high voltage power supply. The pre-cleaned glass substrates were preset to substrate holder. The pressure was maintained inside the chamber is 10^{-5} to 10^{-6} mbar. The required current was increased to evaporate Sn powder. After all, the deposited film was annealed at 500 °C for 1 h in presence of ambient air in the zone furnace.

2.2 Gas Sensing Assets

The gas sensing properties of SnO_2 sensor films were performed by custom fabricated high temperature gas sensing measurement unit. The programmable electrometer (Keithley 6514) was linked to gas sensor unit for the measurement of change in electrical resistance value of sensor i.e. gas response study of SnO_2 sensor. The gas response S (%) of the sensing materials has been designed by the following Eq. (1). The gas response of SnO_2 sensing film has been designed by the well-known relation:

$$Response\ (S\,\%) = \frac{(R_{air} - R_{gas})}{R_{air}} \times 100, \qquad (1)$$

where R_{air} and R_{gas} represent the resistances of sensor in the presence of fresh air and NO_2 gas, respectively.

3. RESULTS AND DISCUSSION

3.1 Raman Analysis

Raman analysis is carried out to determine the appearances of SnO_2. The Raman spectra of SnO_2 sensor film is as shown in Fig. 1.With rutile structure of SnO_2 belongs to the point group D_{4h} with two SnO_2 molecules

* drvbpatil@gmail.com

per unit cell and 15 optical phonons analogous to this symmetry as given by:

$$G_{rutile} = A_{1g} + A_{2g} + A_{2u} + B_{1g} + B_{2g} + 2B_u + E_g + 3E_u, \quad (2)$$

where the modes of A_{1g}, B_{1g}, B_{2g} and E_g symmetry are Raman active [12, 13].

The spectra of SnO_2 shows three peaks at 473, 630, and 773 cm^{-1} out of the four fundamental Raman-active peaks corresponding to the rutile structure of SnO_2. These Raman peaks correspond to the E_g, A_{1g}, and B_{2g} vibration modes, respectively [14]. A_{1g} and B_{2g} modes are allied with the expansion and contraction vibration mode of Sn–O bonds and E_g mode corresponding to the vibration of oxygen [15]. There are two weak Raman lines at 543 cm^{-1} and 691 cm^{-1} in Fig. 1. The appearance of the band at 691 cm^{-1} might correspond to the IR active modes longitudinal optical (LO) phonons of A_{2u} modes [16]. The weak Raman band of 543 cm^{-1} was a consequence of the disorder activation. Another probable reason might be that the oxygen vacancies induced the Raman activity [17]. Thus, the presence of oxygen vacancies in SnO_2 is confirmed by Raman analysis.

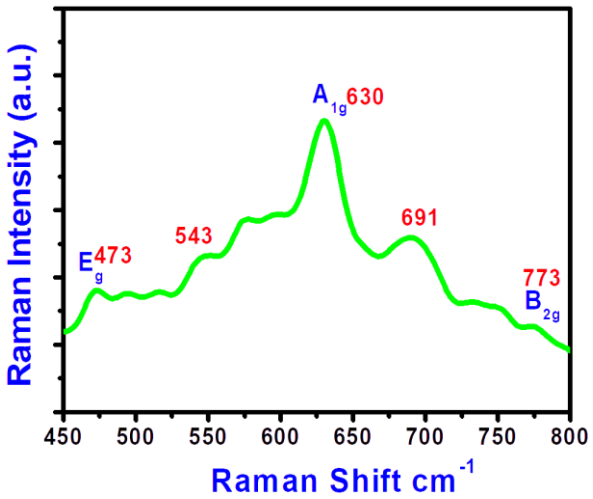

Fig. 1 – Raman spectra of SnO_2

3.2 Morphological Analysis

The scanning electron microscopy (SEM) of prepared SnO_2 film is shown in Fig. 2a. From SEM micrographs uniform nanostructure was revealed. The nanostructure was observed to be uniform and crack (surface defect) free, which is favorable for the gas sensing applications as it increase the adsorption of gas molecules on the sample surface. The chemical composition of SnO_2 thin film was examined by energy dispersive analysis by X-ray (EDAX) spectroscopy and is shown in Fig. 2b. The elemental content and weight percentage is shown in documented as inset table in Fig. 2b. The EDAX result indicated the presence of Sn and O elements. However, the absence of any other peak except those due to Sn and O supported the formation of SnO_2 films without any other elemental impurities.

The 2D and 3D AFM topographs of the SnO_2 film are as shown in Fig. 2c and Fig. 2d. The topographs showed high degree of hills and valley suggesting porous nature of as-grown thin film surface. The RMS roughness of 102 nm is confirmed from the 3D AFM image of SnO_2. The highly rough surface increases the effective area for the adsorption and desorption of gases which thus helps in improving gas sensing properties.

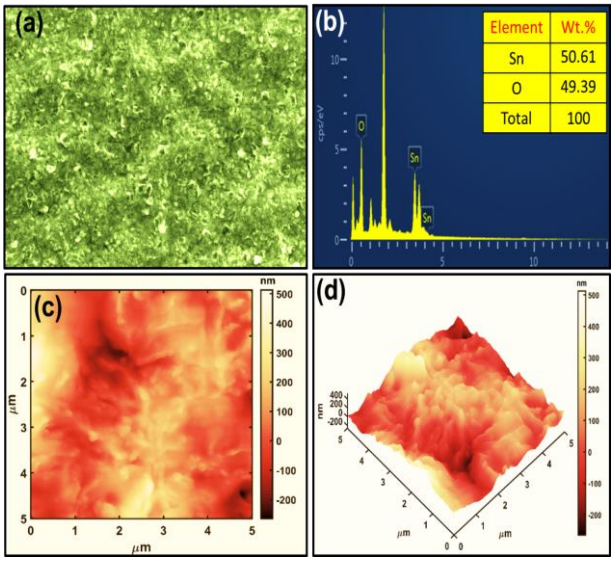

Fig. 2 – SEM (a), EDAX (b), 2D (c) and 3D (d) AFM images of SnO_2 sensor film

3.3 Gas Sensing Study

The ability of a sensor film to respond to a certain gas in presence of other test gases is called as selectivity and it is a very vital factor for marketable gas sensors. Therefore, for selectivity study, initially the sensing performance of SnO_2 thin films towards fixed 100 ppm concentration of various toxic gases were studied and the corresponding results are shown in Fig. 3a. Selectivity graph clearly indicate that the SnO_2 sensor film was more sensitive towards NO_2 gas as compare with other test gases such as LPG, H_2S, Cl_2 and methanol this is due to the rate of reaction between SnO_2 sensor surface and NO_2 gas molecules is much faster.

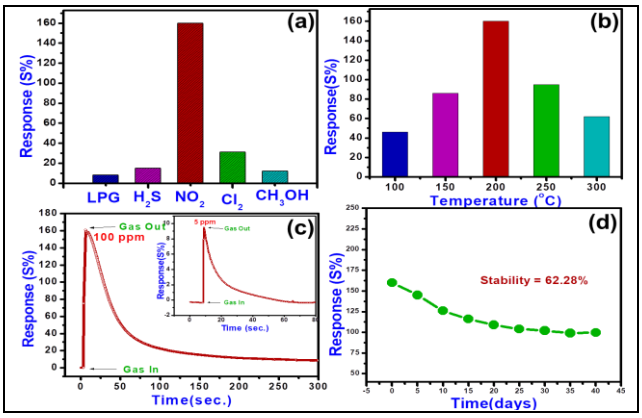

Fig. 3 – Selectivity study (a), temperature dependence (b), response curve (c) and stability study of SnO_2 (d)

In gas sensing study the operating temperature is vi-

tal factor, which manipulates the adsorption/desorption process of oxygen ions on the surface of the sensor film, to optimize operating temperature of tin oxide sensor film the gas sensing measurement were performed at different temperature ranges from 100 °C to 300 °C. From Fig. 3b it is clear that, SnO_2 sensor film shows highest response of 160 % for 100 ppm of NO_2 gas at 200 °C compared to other operating temperature. So further gas sensing study carried out at 200 °C operating temperature.

Fig. 3c shows response curve of SnO_2 sensor for the concentration of 100 ppm and 1 ppm of NO_2 gas as a function of time at optimal operating temperature of 200 °C. The SnO_2 sensor shows maximum response of 160 % at 100 ppm NO_2 gas, while sensor shows response of 9 % on exposure at 5 ppm of NO_2 gas. This is because, at high concentration of NO_2 gas (i.e. 100 ppm) gas covers larger surface area and more active sites are existing at SnO_2 sensor film due to this surface reactions with NO_2 gas molecule increases. At low concentration (i.e. 1 ppm) gas covers comparatively minimum surface area hence less surface reactions occurs on SnO_2 sensor surface and exhibits lower response [19]. The stability study of SnO_2 sensor was measured for 40 days on exposure of concentration of 100 ppm NO_2 gas at 200 °C. The results obtained from stability study are depicted in Fig. 3d. The SnO_2 sensor shows stability of 62.28 %. This decrease in the response of SnO_2 sensor may be due to effect of aging.

4. CONCLUSIONS

The SnO_2 sensor films were fabricated on glass substrates by simple catalyst free thermal evaporation method. SnO_2 sensor gives really high response with very fast response and recovery time, admirable selectivity, good stability as well in response at 200 °C working temperature. The SnO_2 sensor show highest response of 160 % on coverage of 100 ppm NO_2 gas. From the obtained gas sensing results we faith that, as-prepared SnO_2 sensors are proficient for gas sensing applications in industrial zone.

REFERENCES

1. S. Maeng, S.W. Kim, D.H. Lee, S.E. Moon, K.C. Kim, A. Maiti, *ACS Appl. Mater. Interf.* **6**, 357 (2014).
2. B. Wang, L.F. Zhu, Y.H. Yang, N.S. Xu, G.W. Yang, *Phys. Chem. C* **112-117**, 6643 (2008).
3. M.R. Vaezi, M. Zameni, *Ceram. Proc. Res.* **13**, 778 (2012).
4. K.S. Shamala, L.S. Murthy, K.N. Raao, *Mater. Sci.* **27**, 295 (2004).
5. D. Khanh, N.T. Binh, N.N. Long, D.H. Chi, K. Higashimine, T. Mitani, *Korean Phys. Soc.* **52**, 1689 (2008).
6. D. Leng, L. Wu, H. Jiang, Y. Zhao, J. Zhang, W. Li, L. Feng, *Photoenergy*, 1 (2012).
7. K.S. Shamala, L.S. Murthy, K.N. Rao, *Bull. Mater. Sci.* **27**, 295 (2004).
8. Y. Liu, E. Koep, M. Liu, *Chem. Mater.* **17**, 3997 (2005).
9. J. Kaur, S.C. Roy, M.C. Bhatnagar, *Sensor. Actuat. B* **123**, 1090 (2007).
10. C. Liangyuan, B. Shouli, Z. Guojun, L. Dianqing, C. Aifan, C.C. Liu, *Sensor. Actuat.* **134**, 360 (2008).
11. J. Wöllenstein, H. Böttner, M. Jaegle, W.J. Becker, E. Wagner, *Sensor. Actuat. B* **70**, 196 (2000).
12. R.S. Katiyar, P. Dawson, M.M. Hargreave, G.R. Wilkinson, *Phys. C: Solid State Phys.* **4**, 2421 (1971).
13. J.X. Zhou, M.S. Zhang, J.M. Hong, Z. Yin, *Solid State Commun.* **138**, 242 (2006).
14. R.N. Mariammal, K. Ramachandran, B. Renganathan, D. Sastikumar, *Sensor. Actuat. B* **169**, 199 (2012).
15. K.N. Yu, Y. Xiong, Y. Liu, C. Xiong, *Phys. Rev. B* **55**, 2666 (1997).
16. L. Abello, B. Bochu, A. Gaskov, S. Koudryavtseva, G. Lucazeau, M. Roumyantseva, *Solid State Chem.* **135**, 78 (1998).
17. A. Di, A. Romano, A. Vil, J.R. Morante, *Appl. Phys.* **90**, 1550e7 (2001).
18. D.K. Bandgar, S.T. Navale, Y.H. Navale, S.M. Ingole, F.J. Stadler, N. Ramgir, D.K. Aswal, S.K. Gupta, R.S. Mane, V.B. Patil, *Mater. Chem. Phys.* **189**, 191 (2017).